
Liquid Crystals
Publication details, including instructions for authors and subscription information:
http://www.tandfonline.com/loi/tlct20

# An effective method for evaluating the image-sticking effect of TFT-LCDs by interpretative modelling of optical measurements

Po-Lun Chen [a] , Shu-Hsia Chen [a] & Feng-Cheng Su [b]

[a] Institute of Electro-Optical Engineering, National Chiao Tung University, 1001 Ta Hsueh Road, Hsinchu 300, Taiwan, ROC

[b] Unipac Optoelectronics Corporation, 3 Industry E. Road 3, Science-Based Industrial Park, Hsinchu 300, Taiwan, ROC

Published online: 06 Aug 2010.

To cite this article: Po-Lun Chen , Shu-Hsia Chen & Feng-Cheng Su (2000) An effective method for evaluating the image-sticking effect of TFT-LCDs by interpretative modelling of optical measurements, Liquid Crystals, 27:7, 965-975, DOI: 10.1080/02678290050043923

To link to this article: http://dx.doi.org/10.1080/02678290050043923

LIQUID CRYSTALS, 2000, VOL. 27, NO. 7, 965–975

# An effective method for evaluating the image-sticking effect of TFT-LCDs by interpretative modelling of optical measurements

PO-LUN CHEN*, SHU-HSIA CHEN

Institute of Electro-Optical Engineering, National Chiao Tung University, 1001 Ta Hsueh Road, Hsinchu 300, Taiwan, ROC

and FENG-CHENG SU

Unipac Optoelectronics Corporation, 3 Industry E. Road 3, Science-Based Industrial Park, Hsinchu 300, Taiwan, ROC

(*Received 2 August 1999; in final form 21 February 1999; accepted 22 February 1999*)



The conventional method of evaluating the image-sticking effect of a LCD module is inspection by sight, because the residual optical difference between two stressing areas is small and viewing angle-dependent, so that it is difficult to obtain a significant optical difference value by instrumental measurement. We propose an effective method for evaluating the image-sticking effect of a TFT-LCD module by directly measuring its time evolution of transmission with the TFT glass turned off after a period of pattern stress. In this way, the liquid crystal system under charge equilibrium in constant-charge mode shows a dramatically amplified optical difference. Further, we interpret the measured results by a modelling that combines the calculation of liquid crystal director orientation and ionic charge distribution. It is supposed that there are four time constants that dominate the overall sticking phenomenon and belong to four transient processes: adsorption of ions, desorption of free ions, desorption of stuck ions, and TFT leakage. The modelling shows good accordance between measured and simulated results when fitting parameters are properly chosen.

## 1. Introduction

Thin film transistor liquid crystal displays (TFT-LCDs) have provided the main stream of large size liquid crystal displays. With new optical modes and advancing technology, LCDs are being made which achieve the goals of wide viewing angle, high contrast ratio, fast response time, and low power consumption. However, image stability is also required for modern LCDs. It is necessary to consider the problems of flicker [1], cross-talk [2], and image-sticking effect [3] in improving the qualities of LCDs.

After a static image has been displayed on a LCD for a long period of time, the image remains while displaying the next one. This phenomenon is the so-called image-sticking effect or image-retention, and has been considered to result from ionic charge effects. However, LCDs under an a.c. drive can avoid ionic charge effects, although the alignment layer conditions in both sides are different [4]. Generally speaking, it is easy to eliminate the d.c. voltage component across the LC layer by adjusting the d.c. level of the common electrode. Unfortunately, the d.c. voltage component cannot remain constant with respect to variation of grey-level in TFT-LCDs. That is, areas with different grey-levels introduce different LC capacitance values, so that the d.c. offset due to the capacitance coupling effects of TFT-LCDs [3] is also different in each area. Accordingly, one can no longer find a common d.c. level to eliminate the d.c. voltage component. Hence the image-sticking effect in TFT-LCDs is much more severe than in other LCDs.

Ionic charge effects have been widely studied by using voltage, current, capacitance, and optical measuring techniques. Electrical measuring techniques give a more sensitive variation in measured results when impurity ions transport; optical measurements give a directly observable optical performance. Voltage measurement techniques include voltage holding ratio (VHR) measurement [5], and dielectric absorption method for residual d.c. voltage measurement [6]. The VHR is measured to evaluate the holding capacity of a LC cell on which the combination of LC and alignment layer (AL) plays an important role. The dielectric absorption method can give an index (residual d.c. voltage) to evaluate the image-sticking effect of a LC cell.

The measurement of transient current can be used to investigate the leakage current flowing in LCDs and

*Author for correspondence; e-mail: u8424809@cc.nctu.edu.tw

gives a useful way of obtaining the LC resistivity [7]. Measurement of capacitance gives an effective means of analysing the LC director orientation and the distribution and motion of ionic charge. Examples include studies by measuring the C–V characteristics in a d.c. electric driving field [8], the time response of a LC cell in a switched d.c. electric field [9], and dielectric properties of LCs in the ultralow frequency regime [10].

Optical measurement studies always discuss the image problems of LCDs such as flicker, cross-talk, and image-sticking effect; for example, the optical response of LC cells to a low frequency driving voltage [11]. However, these studies focused on indium tin oxide (ITO) cells that cannot properly yield the practical characteristics of TFT-LCDs; few of them directly investigated the image-sticking effect. To observe an image-sticking phenomenon, in fact, implies distinguishing the transmission difference between areas in a retained image. This retained image is the same pattern as the previous displayed one, but visually obscure. Most conventional methods for analysing the image-sticking effect, as listed in table 1 [6, 12–15], always use ITO test cells; each specific driving scheme is designed to obtain clear measuring parameters as evaluating indices. Up to now, it is difficult to find a method for optical measurement of a LCD module showing a clearly distinguishable residual pattern. Accordingly, the LCD modules are inspected by sight to evaluate the image-sticking effect in the present industrial application.

In this paper, we propose an effective method for evaluating the image-sticking effect of TFT-LCDs by direct optical measurement on modules. We also proposed a modelling to analyse the measured results and discussed the behaviour of ions in the TFT-LCD module. When measuring the optical properties of a TFT-LCD module instead of an ITO cell, extra consideration must be given to the driving scheme (such as line-inversion technique) in the TFT-LCD module. In addition, we must consider the d.c. voltage component across the LC layer due to capacitive coupling effects.

The time evolution of transmission was first observed by turning the TFT gates off. Using this driving method as the testing pattern in this work, the gate-off method (GOM) ensures that the whole LC system under the charge equilibrium is in constant-charge mode, giving a dramatically amplified optical difference between different sticking areas. A discontinuity in the time evolution of transmission characteristics was also observed at the switching moment when the stressing pattern was turned to the testing pattern. Modules with different stressing time, ambient temperature, and material combination of LC and AL were measured for comparison. A modelling was proposed to interpret further the implications of the experimental observations. It is supposed that there are four time constants that dominate the overall image-sticking phenomenon in a TFT-LCD module, belonging to four transient processes: adsorption of ions, desorption of free ions, desorption of stuck ions, and TFT leakage. Each transient process contributes to a different sticking phenomenon. Good accordance between measured and simulated results is obtained by properly choosing the fitting parameters.

## 2. Measurement set-up and TFT-LCD module preparation

### 2.1. *Measurement set-up*

The use of TFT-LCD modules with a formal driving scheme is the primary consideration in our measurement set-up. It is also necessary to obtain easily distinguishable grey-levels in a retained image.

Table 1. Methods for evaluation of the image-sticking effect.

| Method | Technique | Cell/panel/ module | Stressing d.c./ voltage | Stressing a.c./ freq./voltage | Stressing time | Disadvantage |
|---|---|---|---|---|---|---|
| 1 | Direct optical measurement | ITO cell | 1 V | 1 kHz/$V_{50}$ | 10 min | ITO cell measurement, not real module. |
| 2 | Direct optical measurement | Panel | 0.25 ~ 2 V | NA | 8 h | Short sticking time; obscure residual pattern. |
| 3 | Direct optical measurement | Specific module | 2/0.4 V | NA | 4 h | Removing $C_{st}$ of TFT to increase d.c. component. |
| 4 | Flicker minimizing method | ITO cell | − 2 ~ + 2 V | 30 Hz/3.0 V | 30 min | Same as in 1. |
| 5 | Dielectric absorption method | ITO cell | 10 V | 30 Hz/2.4 V | 1 h | Same as in 1; residual d.c. voltage, not residual transmission. |
| GOM | Direct optical measurement | Module | (± 0.1 + 0.8) V | 60 Hz/$V_{10}$, $V_{90}$ | 1 h or less | Affected by TFT characteristics. |

Our set-up is depicted in figure 1 (*a*). A LCD module is driven by signals from a video signal generator (Astrodesign, Inc. VG-827). Two image patterns were first set in the programmable memory of VG-827. These patterns are described as follows:

(1) A window pattern with a white rectangular region within a surrounding black region, as shown in figure 1 (*b*), is used as the stressing pattern; this is displayed in the stressing period for a long period of time before observation of the retained image. Because the white level and the black level introduce difference d.c. voltages to their corresponding pixels, and the d.c. difference between these two levels is larger than that between any other two levels, a pattern simultaneously offering a white region and a black region with a significant area could be the stressing pattern. Thus, other patterns, such as two side-by-side white and black regions, can also be used as the stressing pattern.

(2) This, denoted as the testing pattern, may increase the contrast of retained images which become distinguishable. The driving signal from VG-827, in fact makes the gates of all TFTs turn off during the whole testing period. However, we still call it a pattern. In this way, a.c. and d.c. signals are no longer applied to the LC layer.

The stressing and testing patterns described above will be referred to below as pattern 1 and 2, respectively. For measurement, pattern 1 was displayed for a period of time, and then changed to pattern 2 at $t = 0$. We used a luminance meter (Topcon BM-7) to measure the transmission of each area in the window pattern when either patterns 1 or 2 were displayed.

### 2.2. *TFT-LCD module preparation*

Four 6.1 inch (diagonal) and normally white TFT-LCD modules within $640 \times 480$ pixels under the line-inversion drive system were prepared for these measurements. There are 6 bits of data in each red, green, and blue colour. This implies 64 levels in each colour. Level 0 and level 63 will be referred to below as white state and black state, respectively. Different combinations of LC and AL were used in these modules. Four modules are referred to below as module 1 (one of the Unipac's recipes), module 2 (AL: Nissan SE-7091/LC: Chisso 5020), module 3 (AL: Nissan SE-7068/LC: Chisso 5020), and module 4 (AL: Nissan SE-7068/LC: Merck 6252). The thickness of AL was 0.1 μm and the cell gap was $4.85 \pm 0.05$ μm.

Before measurement, the driving signals of each module were adjusted as described below. All the signals were monitored by an oscilloscope. At first, the d.c. voltage level of the common signal denoted as $V_{c,dc}$ was calibrated to eliminate the d.c. component across the LC layer according to the middle grey level (level 32). Thus, the d.c. values across the LC layer were negative (say, $-0.1$ V) and positive (say, 0.1 V) according to the white level (level 0) and the black level (level 63), respectively. This introduced almost equal ionic charge effects since the absolute values of $\pm 0.1$ V are the same. Next, we intentionally adjusted $V_{c,dc}$ down a value of 0.8 V,

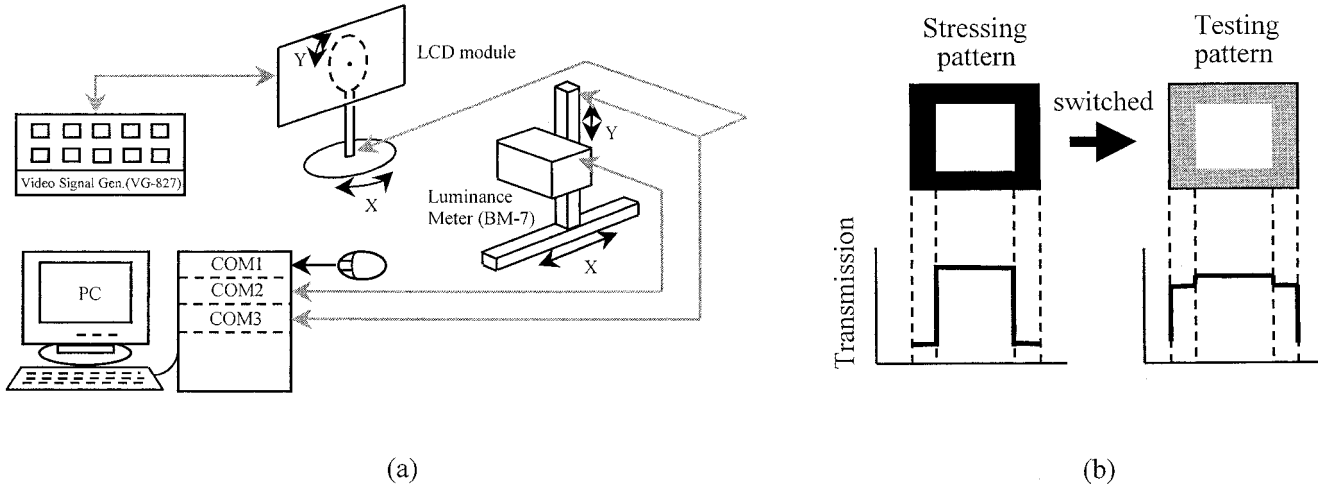


Figure 1. (*a*) The set-up for the gate-off method in which the luminance meter is moved in the $x$ direction to receive the transmission of each area in a TFT-LCD module. (*b*) The stressing pattern is a window pattern with a white inside and black surround.

defined as $\Delta V_{c,dc}$, to enhance the ionic charge effects in the measurement. Finally, we began the measurement by the BM-7 that recorded the transmission from the fixed position in area 1 and area 2 in a time step.

## 3. Measured results

### 3.1. *T–t curves under different ambient temperatures*

Figure 2 shows the time dependence of normalized transmission ($T$–$t$ curve) for module 1 with 60 min pattern-stress, under different ambient temperatures. The time at $t = 0$ represents the moment when pattern 1 is switched to pattern 2; that is, the time between the stressing period and the testing period. The dashed line and the solid line indicate the $T$–$t$ curve in the white stressing area (denoted area 1) and black stressing area (denoted area 2), respectively. A discontinuity in the time evolution of transmission characteristics was observed at $t = 0$. We define the difference of transmission between area 1 and area 2 at $t = 0$ as $\Delta T$, see figure 2 (*a*). However, after the module had been stressed by pattern 1, a significantly large $\Delta T$ was obtained on switching the image to pattern 2.

It was clearly found that a higher stressing temperature introduced a larger difference of transmission between area 1 and area 2 as well as a larger $\Delta T$. That is, a higher stressing temperature introduced a larger difference of accumulated ionic charge in between. The transmissions in area 1 at $t = 0$ defined as $T_W$ remained almost constant under different ambient temperatures, while transmissions in area 2 at $t = 0$ defined as $T_B$ varied with ambient temperature. With time, the optical difference between these two areas became smaller. The transmission in each area gradually changed toward the normally white level, with a changing rate defined



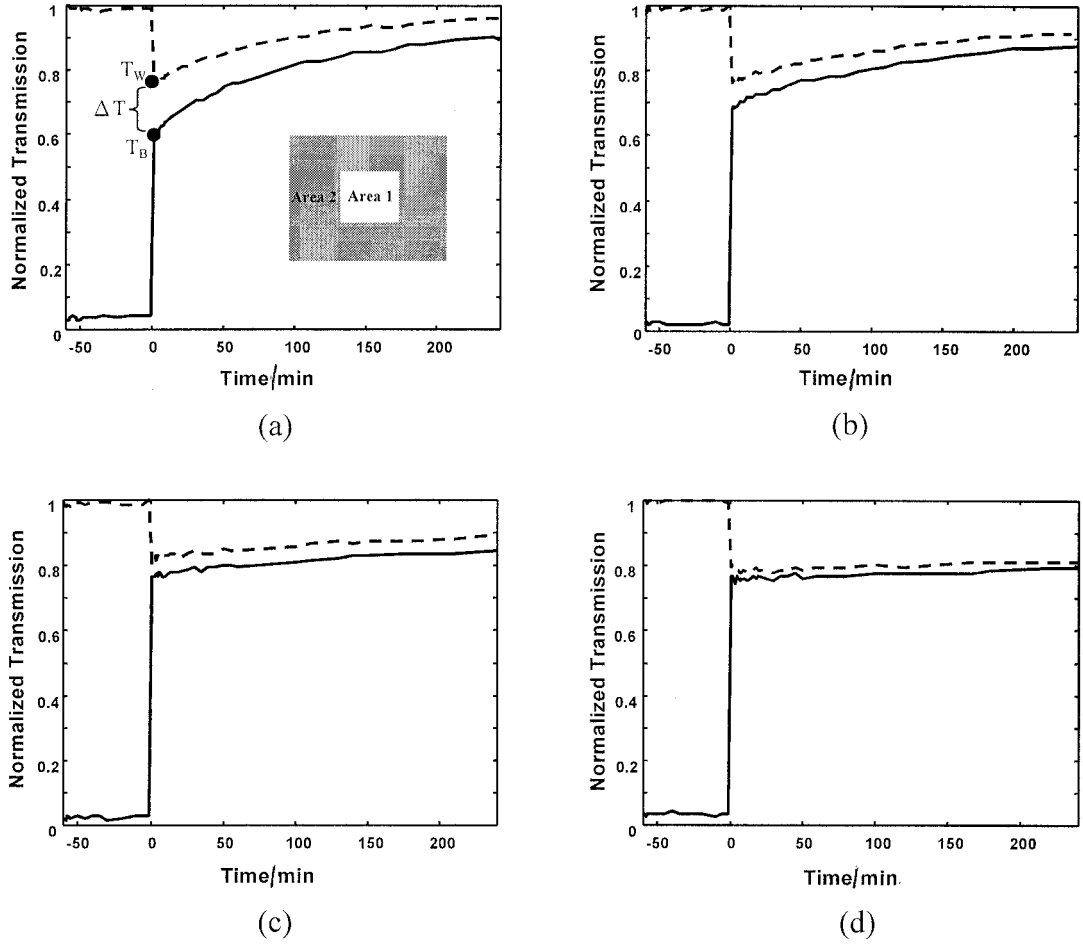


Figure 2. The time dependence of normalized transmission ($T$–$t$ curve) for the module 1 with 60 min stressing under different ambient temperatures (both stressing and testing temperature): (*a*) 60°C, (*b*) 50°C, (*c*) 40°C and (*d*) 30°C. The time at $t = 0$ represents the moment when pattern 1 is switched to pattern 2. The dashed line and the solid line indicate the $T$–$t$ curve in the white stressing area (area 1) and black stressing area (area 2), respectively. We define the difference of transmission between area 1 and area 2 at $t = 0$ as $\Delta T$.

as $R$ in the $T$–$t$ curve. It was found that a higher temperature leads to an increased rate of change. $\Delta T$ and $R$ are the two primary indices for evaluating the image-sticking effect. The former indicates the optical difference between two areas, while the latter indicates the speed of disappearance of the residual image.

### 3.2. *T–t curves with different stressing times*

Figure 3 shows the $T$–$t$ curves for module 1 under an ambient temperature of 60°C, with different stressing times. It is seen that the longer the stressing time, the larger the difference of transmission between areas 1 and 2 as well as $\Delta T$. That is, a longer stressing time introduces a larger difference of accumulated ionic charge in between. With time, the optical difference between these two areas became smaller, but the rate of change $R$ remained almost the same with different stressing times. Comparing the results of figures 2 and 3, it can be seen that the rate $R$ is influenced by ambient temperature, but not by stressing time. However, both the stressing time and ambient temperature influence the accumulated ionic charge on the LC and AL interfaces as well as $\Delta T$.

### 3.3. *T–t curves with different combinations of LC and AL*

Figure 4 shows the $T$–$t$ curves for modules 1, 2, 3 and 4, stressed for 60 min under an ambient temperature of 60°C. Each module gives quite different $T$–$t$ characteristics due to the different combination of LC and AL. It was found that $T_W$, $T_B$ and $\Delta T$ were obviously different for all modules. In modules 3 and 4, where the AL material SE-7068 was used, it was found that both gave a very small $\Delta T$. This may be because the AL of SE-7068 is liable to saturate when it traps ionic charge. Further stressing time cannot introduce more accumulated ionic charge after saturation, so that the accumulated quantities under white-stress and black-stress are almost the same, as well as the $\Delta T$. However, an AL with such a property



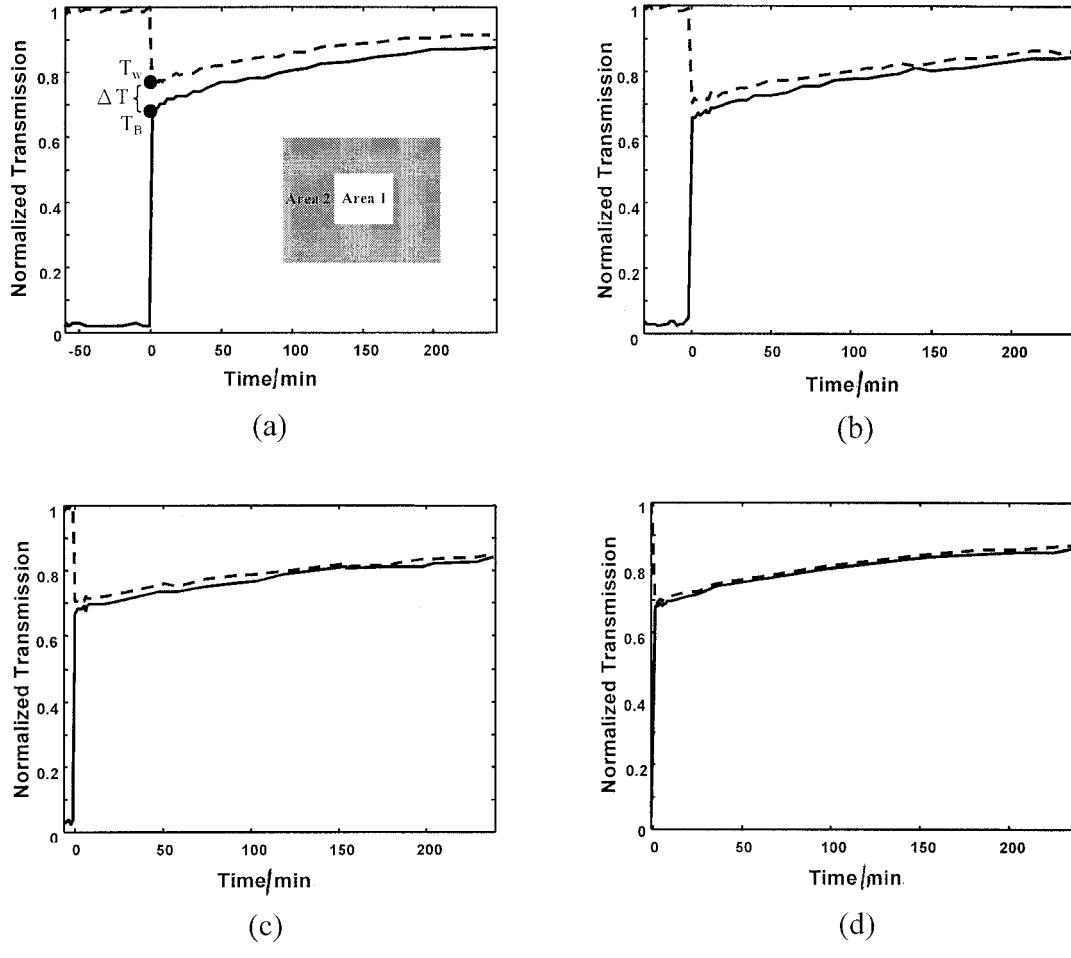


Figure 3. The time dependence of normalized transmission ($T$–$t$ curve) for the module 1 under an ambient temperature of 60°C, with different stressing times: (*a*) 60 min, (*b*) 30 min, (*c*) 5 min and (*d*) 1 min. The time at $t = 0$ represents the moment when pattern 1 is switched to pattern 2. Lines and $\Delta T$ as for figure 2.

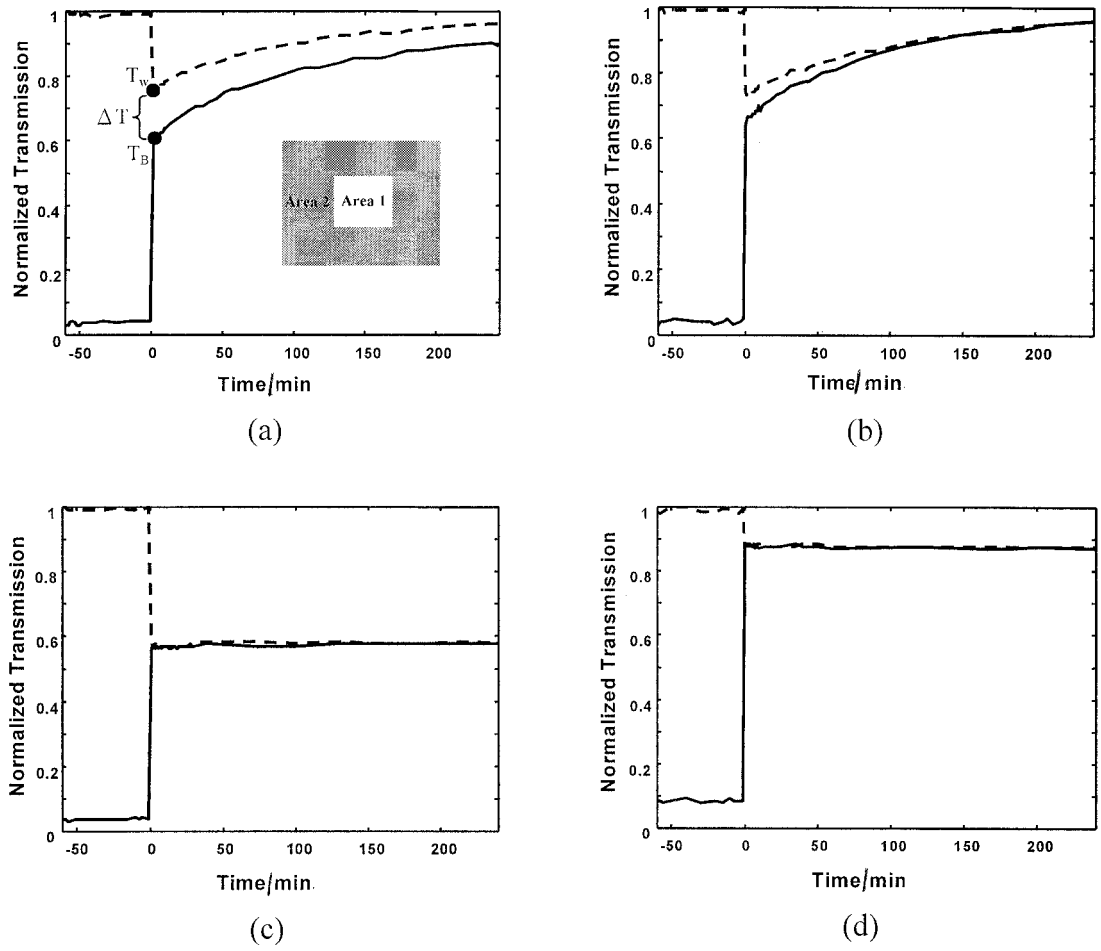


Figure 4. The $T$–$t$ curves for modules 1 (*a*), 2 (*b*), 3 (*c*) and 4 (*d*) stressed for 60 min under an ambient temperature of 60°C. The time at $t = 0$ represents the moment when pattern 1 is switched to pattern 2. Lines and $\Delta T$ as for figure 2.

is beneficial in reducing the optical difference in the image-sticking effect. Another similar tendency found in both modules 3 and 4 is the slow rate of change $R$. This may account for the large trapping force of an AL of SE-7068, so that the equilibrium process of charges in the whole TFT-LCD system almost halted.

Although module 2 introduces a larger $\Delta T$ than modules 3 and 4, optical difference between two areas rapidly became smaller with time. This may be accounted for by the small trapping force of an AL of SE-7091, which makes the accumulated ionic charge leave the interface quickly. However, the material combination in module 2 showed a better performance than that in module 1. It is interesting to note that the $T_W$ ($T_B$) level in module 3 was especially low. This phenomenon may result from more accumulated ionic charge in the LC-AL interface, or from a low LC threshold-voltage. To find the correct reason, we therefore discuss this phenomenon by theoretical analysis from the interpretative modelling combining the calculation of LC director orientation and ionic charge distribution.

## 4. Interpretative modelling of the GOM

### 4.1. *Theoretical analysis*

We now further interpret the above discussion by theoretical analysis. We need to consider many complex conditions in analysing a TFT-LCD module, for example, different electric polarities of the a.c. driving signal in different lines (under the line inversion driving scheme), and different d.c. offsets in the areas with different grey-levels. The driving waveforms were observed by oscilloscope to give voltage values for analysis. It should be noted that both a.c. voltage ($V_{ac}$) and d.c. voltage ($V_{dc}$) applied to pixels, influence the orientation of LC, while only $V_{dc}$ influences the ionic charge transportation.

#### *4.1.1. Contribution of d.c. voltage*

In our proposed d.c. model, there are four time constants that dominate the overall image-sticking phenomenon in a TFT-LCD module, associated with four transient processes: adsorption of ions, desorption of free ions, desorption of stuck ions, and TFT leakage.

The image-sticking effect essentially results from the charge equilibrium of these four transient processes. It is also necessary to introduce another two parameters—the probability of stuck ions, and the existing factor of a space charge limit [8]—into the model to explain GOM measurements more completely. The d.c. model for analysing GOM measurements is illustrated in figure 5, where the LC layer is sandwiched by two ALs. The thickness of $AL_1$, LC, and $AL_2$ are $d_1$, $d_{LC}$ and $d_2$, respectively. The dielectric constant of $AL_1$, LC, and $AL_2$ are $\varepsilon_1$, $\varepsilon_{LC}(t)$ and $\varepsilon_2$, respectively. In deriving the analytical equations, the ratio of thickness to dielectric constant in each layer is defined as $D_1$, $D_{LC}(t)$, and $D_2$ respectively.

There are three time periods for the $T$–$t$ characteristics depicted in figure 5(*a*), 5(*b*), and 5(*c*), consecutively.

*(a) The initial state.* The electronic charge densities $\sigma_a$ and $\sigma_d$ form at the moment when the d.c. voltage $V_{dc}$ begins to act on the pixel. The charge densities $\sigma_a$ and $\sigma_d$ are determined by dielectric constants, dimensions of the pixel, and applied voltage; they are of equal quantity but with opposite sign.

*(b) The period of constant voltage mode.* This period is defined as the stressing period when a constant d.c. voltage is acting on the pixel. Since the d.c. electric field dissociates and forces the ionic charge toward the LC and AL interfaces, the absolute values of ionic charge densities, $|\sigma_b|$ and $|\sigma_c|$, increase with time, as do those of the electronic charge densities, $|\sigma_s|$ and $|\sigma_d|$. The d.c. voltage across the LC layer gradually decreases in this period. We assume that the ionic charge densities $\sigma_b$ and $\sigma_c$ are dissociated by the exponential function with time constant $\tau_{adspt}$ and accumulate at the LC–AL interface according to the following equations ($-t_s < t < 0$):

$$\sigma_b(t) = \rho_{SCL} E \times \{1 - \exp[-(t_s + t)/\tau_{adspt}]\} \quad (1)$$

$$\sigma_c(t) = -\sigma_b(t) \quad (2)$$

where $\rho_{SCL}$ ($= V_{dc}/\varepsilon_{LC}$), the space charge limit, represents the theoretical volume charge density that can cause an internal electric field exactly opposite to the applied electric field [7]; $E$ is the existing factor which indicates the maximum ratio of $\sigma_b$ to $\rho_{SCL}$, and $t_s$ is the total stressing time. From Gauss's law, for $|\sigma_a| = |\sigma_d|$ and $|\sigma_b| = |\sigma_c|$, the d.c. voltage across the LC layer $V_{LC}(t)$ is given by

$$V_{LC}(t) = D_{LC}(t)[D_1 + D_{LC}(t) + D_2]^{-1} \times [V_{dc} + \sigma_b(t)(D_1 - D_2)]. \quad (3)$$

The d.c. induced electronic charge densities $\sigma_a$ and $\sigma_d$ are given by

$$\sigma_a(t) = [D_1 + D_{LC}(t) + D_2]^{-1}[V_{dc} - D_{LC}(t)\sigma_b(t)] \quad (4)$$

and

$$\sigma_d(t) = -\sigma_a(t). \quad (5)$$

*(c) The period of constant charge mode.* This period begins at $t = 0$ and is defined as the testing period when the TFT gates are in the off state. The ionic charge densities $\sigma_b(t = 0)$ and $\sigma_c(t = 0)$ finally accumulated in the stressing period are fixed as the initial values in this constant charge period. Without the external applied voltage, the accumulated ionic charge densities $\sigma_b$ and $\sigma_c$ decrease, due mainly to the diffusion effect and the drift effect of the internal electric field across the LC

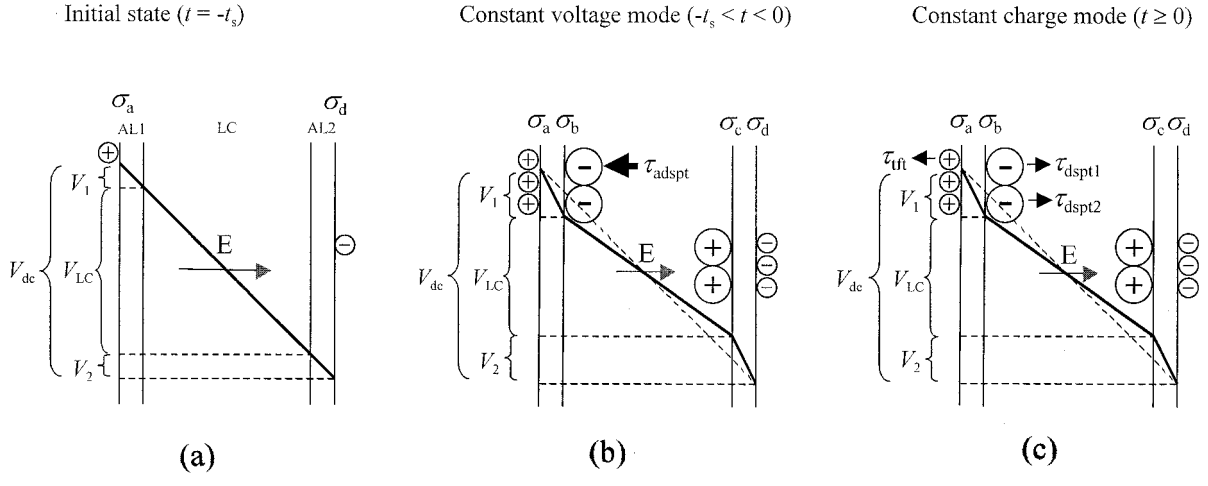


Figure 5. The d.c. model of ionic charge effects in the GOM method. There are three time periods for the $T$–$t$ characteristics: (*a*) the initial state, (*b*) the period of constant voltage mode, and (*c*) the period of constant charge mode.

layer. However, only a portion of the accumulated ionic charge, the 'free ions', leaves the interface rapidly; the portion leaving slowly is defined as the 'stuck ions'. Two voltage components are applied to a LC pixel, the a.c. and d.c. components. 'Free ions' describe ions not trapped at the LC–AL interfaces. Ions that transport back and forth with the alternating electric field (a.c. component) have insufficient time to react with the alignment layers; these are free ions. 'Stuck ions' describe ions trapped at the LC–AL interfaces where they spend a much longer time before leaving the interfaces. The stuck ions are induced only by the unidirectional electric field (d.c. component) that induces ions to react with the LC–AL interfaces and remain there. However, the d.c. component also induces free ions. We assume the free-ions and stuck-ions leave the interface by exponential decay with the time constant $\tau_{dspt1}$ and $\tau_{dspt2}$, respectively. The ionic charge densities of $\sigma_b$ and $\sigma_c$ are determined by the following equations ($t \geqslant 0$):

$$\sigma_b(t) = \sigma_{b0}[(1-P)\exp(-t/\tau_{dspt1}) + P\exp(-t/\tau_{dspt2})] \tag{6}$$

$$\sigma_c(t) = -\sigma_b(t) \tag{7}$$

where $\sigma_{b0}$ is the accumulated ionic charge density $\sigma_b$ at $t = 0$ and $P$ is the probability of stuck ions. In practice, the TFT leakage effect must be considered, though this period is under the constant charge mode. Thus, we assume that the electronic charge densities $\sigma_a$ and $\sigma_d$ leak with the time constant $\tau_{tft}$ as shown in equations (8) and (9), respectively:

$$\sigma_a(t) = \sigma_{a0}\exp(-t/\tau_{tft}) \tag{8}$$

$$\sigma_d(t) = -\sigma_a(t) \tag{9}$$

where $\sigma_{a0}$ is the accumulated electronic charge $\sigma_a$ at $t = 0$. In this testing period, the charge densities $\sigma_a$, $\sigma_b$, $\sigma_c$, and $\sigma_d$ are obtained from equations (6), (7), (8) and (9), respectively. The d.c. voltage across the LC layer can be obtained from

$$V_{LC}(t) = D_{LC}(t)[\sigma_a(t) + \sigma_b(t)]. \tag{10}$$

4.1.2. *Combining the d.c. and a.c. voltage contributions*

We now consider the contribution of $V_{ac}$. By combining the contributions of $V_{ac}$ and $V_{dc}$, the total effective voltage across the LC layer $\hat{V}_{LC}$ is given by

$$\hat{V}_{LC}(t) = D_{LC}(t)\{[\sigma_a(t) + \sigma_b(t)]^2 + \tilde{\sigma}_a(t)^2\}^{1/2} \quad (t_s < t < 0) \tag{11}$$

and

$$\hat{V}_{LC}(t) = D_{LC}(t)[\sigma_a(t) \pm \tilde{\sigma}_a(t) + \sigma_b(t)] \qquad (t \geqslant 0) \tag{12}$$

where $\tilde{\sigma}_a(t)$ is the a.c. induced electronic charge density and is determined from the same equations as in the d.c. case—equation (4) and (8)—by replacing $V_{dc}$ with $V_{ac}$ and letting the ionic charge densities $\sigma_b$ and $\sigma_c$ be zero. It should be noted that the LC dielectric constant ($\varepsilon_{LC}$) is not homogeneous. Thus we must consider the LC director orientation from the Ericksen–Leslie theory in each calculated time step to obtain the effective dielectric constant:

$$\varepsilon_{LC} = d_{LC}\left[\int_{d_{LC}/2}^{d_{LC}/2} \frac{1}{\varepsilon(z)}\mathrm{d}z\right]^{-1} \tag{13}$$

where $\varepsilon(z)$ is the LC dielectric constant at each position $z$, and $d_{LC}$ is the thickness of the LC layer. The dielectric constant $\varepsilon(z)$ is numerically calculated from

$$\varepsilon(z) = \varepsilon_\perp + (\varepsilon_\parallel - \varepsilon_\perp)n_z n_z \tag{14}$$

where $\varepsilon_\parallel$ and $\varepsilon_\perp$ are the dielectric constants parallel and perpendicular to the LC director, respectively, and $n_z$ denotes the $z$ component of the LC director orientation, neglecting the flow effect from the Ericksen–Leslie theory. Also

$$\gamma\frac{\partial n_i}{\partial t} = \frac{\partial}{\partial z}\left[\frac{\partial F}{\partial\left(\frac{\partial n_i}{\partial z}\right)}\right] - \frac{\partial F}{\partial n_i} + n_z(\varepsilon_\parallel - \varepsilon_\perp)\left(\frac{\partial\phi}{\partial z}\right)^2 + \lambda n_i, \quad i = x, y \text{ and } z \tag{15}$$

where $\gamma$ is the rotational viscosity and $\lambda$ is the Lagrange multiplier. $F$, the Helmholtz free energy, given in the vector form [16] is expressed as

$$F = \frac{k_{11}}{2}(\nabla\ \ n)^2 + \frac{k_{22}}{2}\left(\nabla\times n\ \ n + \frac{2\pi}{p_0}\right)^2 + \frac{k_{33}}{2}(\nabla\times n\times n)^2 \tag{16}$$

where $k_{11}$, $k_{22}$, and $k_{33}$ are the Frank elastic constants for splay, twist and bend deformation, respectively. The natural pitch is denoted as $p_0$.

Finally, we use the extended $2\times 2$ Jones matrix method [17] to calculate the optical transmission. In figure 6, the simulated results for all cases in figure 4 can be made to agree with the measurement results by properly choosing or fitting the unknown parameters $\tau_{adspt}$, $\tau_{dspt1}$, $\tau_{dspt2}$, $\tau_{tft}$ and ($PEV_{dc}$). All 22 known parameter values used in the simulation, obtained from either numerical data sheets or from our independent measurements, are listed in table 2.

### 4.2. *Discussion*

In the stressing period, we found that the ionic charges accumulated at the LC–AL interface introduce a certain voltage reduction across the LC layer ($\hat{V}_{LC}$), but with no

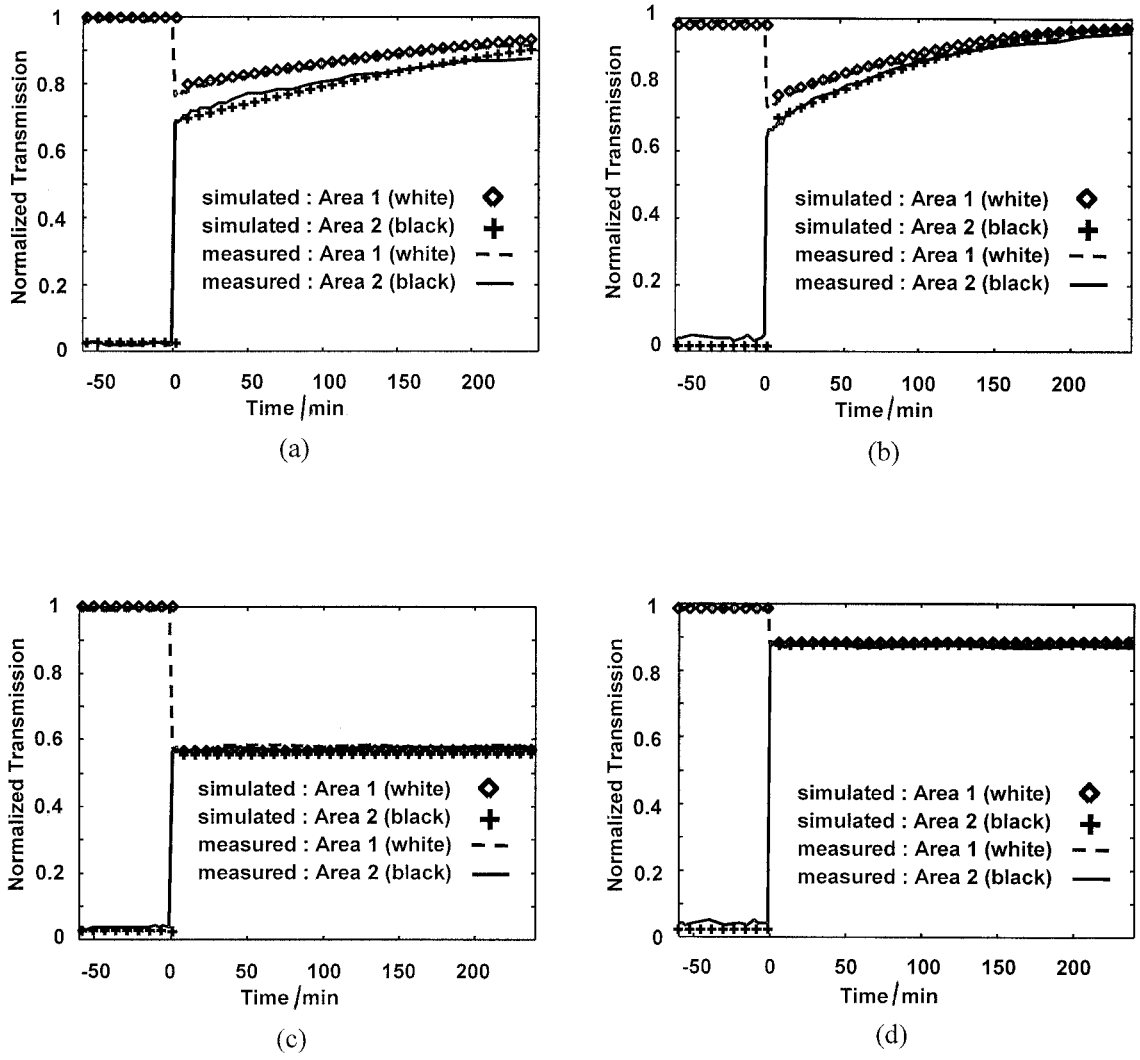


Figure 6. Comparison between measured and simulated results in the case of figure 4. We chose $\tau_{adspt} = 300$ s, $\tau_{dspt1} = 30$ s, and $\tau_{tft} = 30$ s in the simulation. (*a*) Module 1. (*b*) Module 2 with fitting parameters $\tau_{dspt2} = 45\,000$ s, $EP = 0.100$ (white); $\tau_{dspt2} = 40\,000$ s, $EP = 0.082$ (black). (*c*) Module 3 with fitting parameters $\tau_{dspt2} = 9\,000\,000$ s, $EP = 0.111$ (white); $\tau_{dspt2} = 9\,000\,000$ s, $EP = 0.087$ (black). (*d*) Module 4 with fitting parameters $\tau_{dspt2} = 9\,000\,000$ s, $EP = 0.11900$ (white); $\tau_{dspt2} = 9\,000\,000$ s, $EP = 0.09316$ (black).



obvious optical reduction. This reduction of $\hat{V}_{LC}$ is too small to give an obvious variation of transmission in either the white level (level 0) or black level (level 63) curves, as shown in the measured results. Thus, we cannot determine the real value of $\tau_{adspt}$ by the GOM. However, a certain amount of ionic charge is adsorbed at the interface in the stressing period with a speed according to this time constant. Here we let $\tau_{adspt}$ be 300 s in the simulation; since the total stressing time is much longer than 300 s, this arbitrarily but reasonably chosen value has no influence on the initial charge densities for the next (testing) period. The total amounts of accumulated ionic charge play an important role in the succeeding appearance of discontinuity in the time evolution of transmission characteristics at $t = 0$, and in the dramatically amplified optical difference between two areas.

At the moment when TFT gates are turned off at $t = 0$, we consider four kinds of initial charge conditions in a LCD module under the line-inversion driving scheme, say $V_{dc} \pm V_{ac}$ for both area 1 (white) and area 2 (black) in the simulation. Four transient transmission curves, corresponding to the four initial conditions, can be observed after $t = 0$. However, these four transient curves finally aggregate to two curves whose grey-levels are different from those of the two curves in the stressing period. This transient process occurs within a period of a few seconds, very much shorter than the total measuring

Table 2. Parameter values used in this simulation.

| Parameter | | | For figure 4(*d*) | For 4(*b*) and 4(*c*) |
|---|---|---|---|---|
| *Pixel dimension* | | AL1 : $d_1$ | 0.1 μm | 0.1 μm |
| | | LC : $d_{LC}$ | 4.85 μm | 4.85 μm |
| | | AL2 : $d_2$ | 0.1 μm | 0.1 μm |
| *Dielectric constant* | | AL1 : $\varepsilon_1$ | $3\varepsilon_0$ | $3\varepsilon_0$ |
| | | LC : $\varepsilon_{LC}$ | $(3.5 \sim 9.4)\varepsilon_0$ | $(3.2 \sim 8.8)\varepsilon_0$ |
| | | AL2 : $\varepsilon_2$ | $3\varepsilon_0$ | $3\varepsilon_0$ |
| *Liquid crystal parameter* | | $\varepsilon_{\parallel}$ | $9.4\varepsilon_0$ | $8.8\varepsilon_0$ |
| | | $\varepsilon_{\perp}$ | $3.5\varepsilon_0$ | $3.2\varepsilon_0$ |
| | | $n_e$ | 1.5494 | 1.561 |
| | | $n_o$ | 1.4704 | 1.481 |
| | | $k_{11}$ | 14 | 9.6 |
| | | $k_{22}$ | 6.2 | 12.7 |
| | | $k_{33}$ | 21 | 27.7 |
| | | pitch | 25 μm | 62 μm |
| *Pixel voltage in stressing period* ($-t_s < t < 0$) | *Area 1 (white)* | $V_{dc}$ | 0.7 V | 0.7 V |
| | | $V_{ac}$ | ± 0.24 V | ± 0.24 V |
| | *Area 2 (black)* | $V_{dc}$ | 0.9 V | 0.9 V |
| | | $V_{ac}$ | ± 4.2 V | ± 4.2 V |
| *Initial pixel voltage in testing period* ($t = 0$) | *Area 1 (white)* | Positive polarity, the $k_{th}$ line | 0.94 V ($0.7\ V_{dc} + 0.24\ V_{ac}$) | 0.94 V ($0.7\ V_{dc} + 0.24\ V_{ac}$) |
| | | Negative polarity, the $(k+1)_{th}$ line | 0.46 V ($0.7\ V_{dc} - 0.24\ V_{ac}$) | 0.46 V ($0.7\ V_{dc} - 0.24\ V_{ac}$) |
| | *Area 2 (black)* | Positive polarity, the $k_{th}$ line | 5.10 V ($0.9\ V_{dc} + 4.2\ V_{ac}$) | 5.10 V ($0.9\ V_{dc} + 4.2\ V_{ac}$) |
| | | Negative polarity, the $(k+1)_{th}$ line | − 3.30 V ($0.9\ V_{dc} - 4.2\ V_{ac}$) | − 3.30 V ($0.9\ V_{dc} - 4.2\ V_{ac}$) |



time. Thus the measured results show a discontinuity at $t = 0$ because of the larger measurement time scale. However, the d.c. voltages of the LC layer, before and after $t = 0$, obey equations (11) and (12), respectively. It can be intuitively explained that the accumulated ions originating from the a.c. driving voltage $\pm V_{ac}$ disappear in a few seconds after $t = 0$ due to fast leakage of the TFT and the fast desorption of free ions. Note that the process of fast desorption is accompanied by the leakage TFT process.

The time constants $\tau_{dspt1}$ and $\tau_{tft}$ are within the same order of several seconds, but their precise values cannot be determined by the GOM. We reasonably chose $\tau_{dspt1} = \tau_{tft} = 30$ s. for the simulation. However, the residual image occurs due to the slow desorption of stuck ions that are mainly induced by the d.c. component $V_{dc}$. In the GOM, the precise parameter values we need, to determine by fitting the simulated and measured results, are $\tau_{dspt2}$ and $(PEV_{dc})$, which correspond to $R$ and $\Delta T$, respectively. A larger $\tau_{dspt2}$ implies that the stuck ions leave the LC–AL interface more slowly, thus giving a smaller rate of change $R$ in the $T$–$t$ curves. The transmissions $T_W$ and $T_B$ are determined by the surface charge density of stuck ions, $(PE\rho_{SCL})$ $[=(PEV_{dc}/\varepsilon_{LC})]$. In the testing period, the voltage $\hat{V}_{LC}$ [see equation (12)] which introduces the residual image is determined by the charge densities $\sigma_a$, $\tilde{\sigma}_a$, and $\sigma_b$. After several seconds of the transient process due to the fast desorption of free ions and TFT leakage, the remaining charge densities introduce a larger $\hat{V}_{LC}$ difference between areas 1 and 2. This is because $\hat{V}_{LC}$ contains the d.c. component (different in areas 1 and 2) without mixing the large a.c. component (the same in areas 1 and 2). In addition, these $\hat{V}_{LC}$ values correspond to the middle grey-levels so that the GOM allows for a dramatically amplified optical difference.

The index $\Delta T$ used to evaluate the image-sticking effect, indicates the optical difference between two areas. From the simulation, we found that smaller $T_W$ and $T_B$ values result from larger accumulated ionic charge densities $\sigma_b$ or $\sigma_c$. If ionic charge densities $\sigma_b$ or $\sigma_c$ become zero at infinite time, $T_W$ and $T_B$ will become unity. Moreover, we found that $T_W$ and $T_B$ increase as the value of $(PEV_{dc})$ decreases. Also a small $\Delta T$ implies a small difference between $(PEV_{dc})$ values in areas 1 and 2. By fitting the measured and simulated results, the $(PEV_{dc})$ values in area 1, in the cases of figures 4(*b*), 4(*c*)

and 4(*d*), are 0.0700, 0.0777 and 0.0833, respectively. In the same way, the ($PEV_{dc}$) values in area 2, in the same figures are 0.0738, 0.0783, and 0.0838, respectively. From the simulated results, we found that the ($PEV_{dc}$) value in module 3 is lower than that in module 4. The lower $T_W(T_B)$ value in module 3 is due to the low threshold voltage of the LC (Chisso 5020) rather than a higher accumulated ionic charge within. The index $R$ for evaluating the image-sticking effect indicates the speed of disappearance of the residual image. It is found that a smaller rate of change $R$ is due to longer time constant $\tau_{dspt2}$ of stuck ions.

## 5. Summary and conclusion

We have found an effective method for evaluating the image-sticking effect of a TFT-LCD module by directly measuring its time evolution of transmission with the TFT gates turned off after a period of pattern-stress. We interpret the measured results by theoretical analysis. By properly choosing the fitting parameters in our proposed model, these two results are with good accordance. The cases of different ambient temperature, different stressing time, and different combination of LC and AL were measured by this GOM.

We found that high ambient temperature introduces more ionic charge leading to a larger difference of residual transmission, but the accumulated ionic charge is assisted leaving quickly the LC–AL interface. A longer stressing time brings a larger difference of residual transmission. However, the influence of stressing time on the image-sticking effect is smaller than that of ambient temperature.

In our analysis for modules with different combinations of LC and AL, the LC Chisso 5020 is much more pure than other LCs, but its lower threshold voltage may introduce lower $T_W$ and $T_B$ values. The SE-7068 AL is liable to saturation when it traps the ionic charges that originate from the LC bulk. Accordingly, no matter what grey-level shows, it gives almost the same ($PEV_{dc}$) values after a long period of stress; that is, a very small $\Delta T$. The SE-7068 AL introduces small rate of change $R$, so that accumulated ionic charge leaves slowly.

We also inspected the image-sticking effect conventionally by sight after a window pattern had been displayed over 24 h. It showed the same residual tendency as the results measured by GOM. Thus, we can precisely record the measured data and compare with those taken at other times. The GOM helps to eliminate the ambiguity of conventional determinations.

It should be noted that the discussion in this paper can be extended to investigate the residual image phenomenon when the power of a reflective-type TFT-LCD is turned off; in a direct viewing-type TFT-LCD, no residual image is seen because the back light of the module is turned off at the same time.

We wish to thank W.-S. Chang of the Technology Development Division of Unipac Optoelectron. Co. for preparing the TFT-LCD modules, and C.-Y. Yeh of the Quality Management Division of Unipac Optoelectron. Co. for providing measuring supports. Gratitude is also extended to the National Science Council of the R.O.C. for partially providing financial support of this research under Contract No. NSC 88-2212-M-009-030.

## References

[1] Numano, Y., Hayama, M., and Yamazaki, T., 1990, *Jpn. J. appl. Phys.*, **29,** L2384.
[2] Kamagami, S., Sunohara, K., Tanaka, Y., and Morita, H., 1991, *Proc. Int. Disp. Res. Conf.*, 199.
[3] Nagata, S., Takeda, E., Nan-no, Y., Kawaguchi, T., Mino, Y., Otsuka, A., and Ishihara, S., 1989, *SID 89 Digest*, 242.
[4] Kitamura, M., 1996, *Euro Display '96* (Proceedings of International Display Research Conference), 330.
[5] Oh-E, M., and Kondo, K., 1998, *Liq. Cryst.*, **25,** 699.
[6] Manabe, N., and Nakanomatari, J., 1996, *Proc. AM-LCD '96/IDW '96*, LCp 4-1, 237.
[7] Colpaert, C., Maximus, B., and De Meyere, A., 1996, *Liq. Cryst.*, **21,** 133.
[8] Mada, H., and Suzuki, H., 1987, *Jpn. J. appl. Phys.*, **26,** L1092.
[9] Mada, H., and Osajima, K., 1986, *J. appl. Phys.*, **60,** 3111.
[10] Murakami, S., Iga, H., and Naito, H., 1987, *J. appl. Phys.*, **80,** 6396.
[11] Palmer, S., 1998, *Liq. Cryst.*, **24,** 587.
[12] Lien, A., Chen, C.-J., Inoue, H., and Saitoh, Y., 1997, *SID 97 Digest*, 203.
[13] Kanemori, Y., Katayama, M., Nakazawa, K., Kato, H., Yano, K., Fukuoka, Y., Kanatani, Y., Ito, Y., and Hijikigawa, M., 1990, *SID 90 Digest*, 408.
[14] Nanno, Y., Mino, Y., Takeda, E., and Nagata, S., 1990, *SID 90 Digest*, 404.
[15] Sasaki, T., Tsumura, M., Nagae, Y., Suzuki, M., and Iwata, T., 1993, *Trans. IEICE C-II*, **J77C-II,** 392.
[16] Frank, F. C., 1958, *Discuss. Faraday Soc.*, **25,** 19.
[17] Gu, C., and Yeh, P., 1993, *Soc. Am. A*, **10,** 966.